Tribology International 127 (2018) 24–36

Contents lists available at ScienceDirect

Tribology International

journal homepage: www.elsevier.com/locate/triboint

Thermal analysis and tribological investigation on TPU and NBR elastomers applied to sealing applications

B. Pinedo[a,*], M. Hadfield[b], I. Tzanakis[c], M. Conte[d], M. Anand[b]

[a] Ik4- Tekniker, Tribology Unit, Iñaki Goenaga 5, 20600, Eibar, Gipuzkoa, Spain
[b] Bournemouth University, Department of Design and Engineering, Poole, BH125BB, UK
[c] Faculty of Technology, Design and Environment, Oxford Brookes University, Wheatley Campus, Wheatley, OX33 1HX, UK
[d] Anton Paar TriTec SA, Rue de la Gare 4, 2034, Peseux, Switzerland

ARTICLE INFO

Keywords:
Frictional heating
Contact temperature
Polymers
Elastomeric seals

ABSTRACT

This study investigates the contact temperatures reached due to frictional heating on TPU (Thermoplastic polyurethane) and NBR (Nitrile butadiene rubber) seal surfaces during operation. These elastomers present limited thermal resistance so an excessive temperature rise may affect their tribological performance. Sliding tests of the elastomers against steel cylinders were carried out and the surface temperature evolution was acquired during the tests using a high precision infrared camera. Frictional behaviour and temperature curves were analyzed. The influence of the experimental parameters, such as the sealing material, sliding velocity, applied load and steel surface conditions was examined. Experimental thermal results were compared with those calculated through well-established analytical models, in order to determine the advantages and limitations of the latter.

1. Introduction

Elastomeric seals can be found within many mechanical devices such as engines, gearboxes, pumps, flight controllers and a wide range of actuators, among others. Hence, currently there is a wide range of seal geometries and materials that enables their use in several industrial sectors such as automotive, aerospace, manufacturing, and aggressive environments such as off-shore. However, industry is continuously seeking higher performance mechanical components which is a challenge for seal materials researchers due to the limited thermal resistance of the majority of the polymers. In the case of dynamic sealing applications, the temperature to that in-use materials are exposed, is the sum of both the environment and temperature rise caused by the frictional heating. The importance of considering frictional heating effects on sealing applications has been demonstrated by the author [1].

Most of the frictional energy generated during sliding is converted into heat resulting in the temperature rise of the rubbing surfaces. In the case of polymers, their thermal resistance is below 300 °C. The ability to estimate flash temperatures generated under real working conditions of elastomeric components is an important technical issue. Unfortunately, they are still important limitations to continue generating new knowledge concerning the frictional heating phenomena due to the difficulties to measure experimentally the temperatures at the rubbing contact. Many authors have previously used conventional thermocouples, multifunction thin-film thermocouples and techniques involving the detection of IR radiation, among others, in an attempt to measure the temperatures reached during sliding at the interface [2]. Nevertheless, none of these techniques allows measuring the temperature rise at the real contact areas, where the maximum temperatures are reached, and that is why none of those techniques has been widely accepted.

Due to the complexity of obtaining experimental data, many authors have made attempts in the last decades in order to develop analytical models, that resulted in a wide range of equations for estimating the temperature rise at the interface. Some of the most popular models are: Archard's average and maximum flash-temperature model (1959), Holm's average and flash temperature model, Tian-Kennedy's average and maximum temperature model (1993), Greenwood-Greiner's average flash temperature model (1991), Ashby flash temperature model (1991), and Jaeger (1942) and Blok (1937) models, among others [3–8]. Nevertheless, none of these models are able to accurately estimate the contact temperatures at the interface. Furthermore, calculations using different models lead to very different results as demonstrated by Kalin et al. [9]. The main difficulty to develop reliable temperature models is that the surface temperature rise during sliding depends on several factors such as the contact and operating conditions, in addition to the materials and surface conditions of the components.

* Corresponding author.
E-mail address: bihotz.pinedo@tekniker.es (B. Pinedo).

https://doi.org/10.1016/j.triboint.2018.05.032
Received 18 December 2017; Received in revised form 28 March 2018; Accepted 17 May 2018
Available online 19 May 2018
0301-679X/

Moreover, contact conditions will vary considerably during sliding, while several interfacial properties and phenomena are very difficult to model [9]. Hence, most of the theoretical temperature models are based on different physical, dynamic and geometrical assumptions. In particular, a special care should be taken when selecting the contact area to be used for calculations. Even if the contact area significantly affects the results obtained, there are no standard criterion and each model uses different approaches [9]. In the case of polymers, contact temperature estimations are even more complex as their thermo-mechanical properties are strongly influenced by temperature [10–16]. The importance of considering the evolution of material properties in the case of Polytetrafluoroethylene (PTFE) polymers has been already demonstrated [14,15]. In particular, Tzanakis et al. [12] studied the effect of roughness, friction coefficient, contact pressure and velocity on the flash temperatures generated on a PTFE composite elastomer tip seal in contact with a high carbon steel plate under dry sliding conditions. The authors found a specific value of roughness which leads to a higher temperature rise, and that the effect of roughness and sliding velocity was larger than the effect of load. Conte et al. [13] showed the role of frictional heating on the transfer layer regeneration of PTFE composites. PTFE is a semi-crystalline polymer with a melting temperature of about 330 °C and no cross links between the polymeric chains.

The aim of this current study is to investigate how frictional heating affects the tribological properties of TPU and NBR elastomers (having cross linked polymeric chains) during industrial relevant dynamic sealing applications. To this aim, sliding friction tests were carried out on these elastomers under realistic working conditions and the temperature evolution was experimentally measured through a high precision thermo-camera. The tests were carried out at different velocities and surface conditions of the steel mating surfaces, in order to understand to what extent, the different operating parameters affect the temperature rise during operation. Analytical calculations were carried out in order to determine which of the existing models correlate better to the experimental results of these materials as well as their limitations.

2. Experimental procedure

2.1. Test specimens and characterization

In order to reproduce the contact between a stationary elastomeric seal and the moving steel rod at laboratory scale, the cylinder-on-flat configuration was chosen, which approximates the line contact between a differential of seal and its counterface. Fig. 1 presents an image of the cylinder (steel part) and the flat (elastomer) samples. The cylinder samples of diameter 10 mm were made from 42CrMo4V (F1252) steel. The flat samples of L28xW15xT5 mm were made from TPU and NBR.

2.1.1. Thermo-mechanical properties

Prior to the friction tests, the main thermal and mechanical properties of the elastomeric samples were measured. Thermo-mechanical properties of the elastomeric samples at ambient temperature (+25 °C) are shown in Table 1 whereas their diffusivity, conductivity and heat capacity curves are plotted in Fig. 2. The evolution of the heat capacity (Cp) of samples with temperature was measured using DSC 1–500 device (Mettler Toledo, Spain). Dry nitrogen was used for venting at the rate of 50 ml/min. Measurements were carried out in the range between 0 °C and +250 °C. Thermal diffusivity (χ) of samples which expresses its ability to conduct thermal energy relative to its ability to store was measured by means of a high-resolution photopyroelectric calorimeter available at the UPV/EHU (University of the Basque Country), with a test velocity of ± 0.5 °C/min. Based on the heat capacity and diffusivity values, thermal conductivity *(K)* of the samples was calculated as

$$K = \rho\, Cp\, \chi \quad (1)$$

where ρ being the density of the samples which was measured using XP205 precision micro-scale (Mettler Toledo, Spain). Analysis results showed that for both NBR and TPU, the heat capacity and the thermal conductivity increase with temperature whereas the thermal diffusivity decreases. Comparing both plots in Fig. 2, it can be seen that the heat capacity, diffusivity and thermal conductivity of the TPU are lower than those of the NBR. This means that for every one degree rise in temperature in NBR, the heat transfer will be quicker as compared to TPU, i.e. thermal equilibrium will be reached faster in the NBR. In the previous research on PTFE, the authors highlighted the importance of taking into account the variation of thermal properties along temperature [14,15]. In this case, it was seen that such variations along the temperature working range have negligible effect on the calculations. Regarding the steel samples, their properties are also presented in Table 1.

Table 1
Physical properties of the test samples at room temperature (+25 °C).

Property	NBR	TPU	42CrMo4V Steel
Density, ρ (kg/m^3)	1166	1102	7830
Specific heat, Cp (J/g °C)	1.49	1.21	0.5
Diffusivity, χ (m^2/s)	1.5869e^{-7}	1.1005e^{-7}	1.175 e^{-5}
Conductivity, K (W/m K)	0.32	0.15	46
Hardness, H	70 ShA	93 ShA	1000 HV

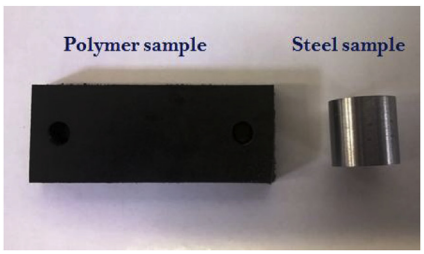

Fig. 1. Tribo-pair selected for the study of the frictional heating phenomenon at laboratory scale.

2.1.2. Surface properties of the test samples

In regard to the steel test samples, cylinders with three different R_a roughness (0.1, 0.2 and 0.5 μm) and surface treatments (chromed and non-chromed plated) were manufactured. Following the recommendations of seal manufacturers, the steel samples were hard chromed-plated with the coating hardness of 1000 HV.

Two and three dimensional surface profiles of the elastomeric samples were measured using a white light interferometer (Zygo Corporation, USA) and the analysis results are presented in Fig. 3. Hardness of the elastomeric samples was measured using a Shore A durometer and its results along with those for steel samples are presented in Table 1. It is acknowledged that the wear of materials and their hardness are related, however, this dependence varies from one material to another. Most of the analytical models for wear estimation predict that the harder the material, the lower is the wear, but in the case of polymers this is not necessarily true [16,17].

2.2. Experimental setup

Tribological sliding tests of the elastomeric flat samples against steel cylinders of different roughness and surface conditions were carried out using TE77 high-frequency sliding machine (Plint Tribology Limited, England) reproducing as close as possible to the common operating conditions of seals made from these materials. The lower sample (elastomer flat) is mounted on a reciprocating arm connected to an electric motor which provides linear motion. The upper sample (steel cylinder) is connected to a load cell that records instantaneous kinetic friction force generated during motion at prescribed time intervals.

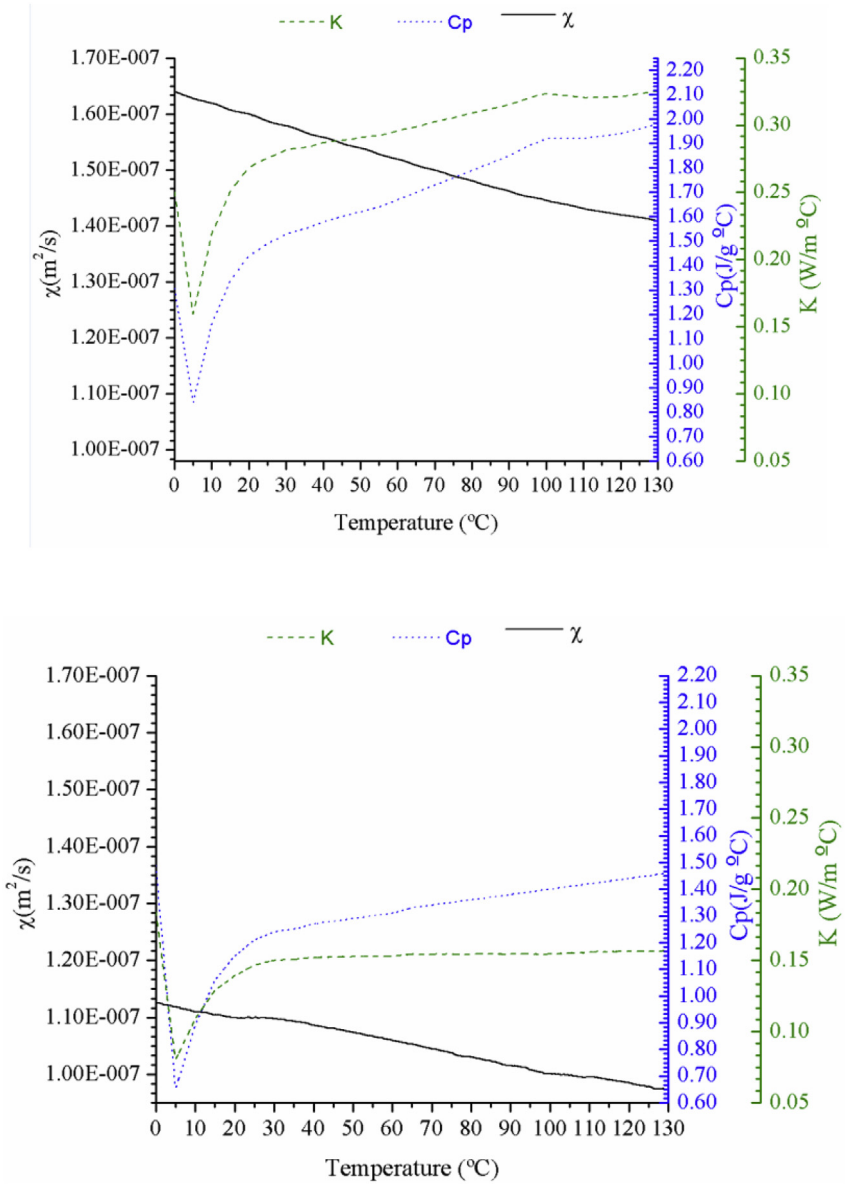

Fig. 2. Thermal properties of the test samples: (a) NBR and (b) TPU.

Fig. 4 shows a view of the cylinder-on-flat configuration and test assembly. The elastomeric sample is loaded against the steel cylinder (held in a holder) by means of a spring loading mechanism.

Friction tests were carried out under dry sliding conditions at room temperature. A stroke length of 5 mm and a normal load of 15 N were used. The maximum operating velocity recommended by manufacturers for seals made from these materials is 0.5 m/s, and the main reason for the velocity constraint is the low temperature resistance of these materials (approximately 100 °C). In this study, tests were carried out at sliding velocities of 0.1 and 0.25 m/s. During each test coefficient of friction and surface temperatures were recorded, and each test was repeated at least two times. Test conditions are summarized in Table 2.

During the sliding tests the temperature field on the tribo-pair was measured and acquired by means of a Flir SC300 high precision thermocamera (FLIR systems, Inc.). In Fig. 5 a complete image of the TE77 test rig and the infrared camera assembly is shown. The camera measures and visualises the infrared radiation emitted from an object which varies with temperature and radiation wavelength. As the radiation is a function of the surface temperature of objects, it is possible for the camera to calculate and display this temperature. The radiation measured by the camera also depends on the object emissivity. The camera used in this investigation operates within the spectral range of 8–9 μm and has a measurement range from −20 °C to +2000 °C.

The camera was installed at a distance of 100 mm from the contact interface of the tribo-pair to maintain focus. The accuracy of the camera is of ± 1% or ± 1 °C for the measurement range used in the current study (25 °C to 150 °C). The infrared camera system has a sensitivity of 20 mK at 30 °C and a resolution of 320 × 240 pixels. Calibration of the camera was carried out following the procedure described by its manufacturer. In particular, the system was calibrated by determination of emissivity (ε) of the target objects and calibrating to the environmental temperature for each test. For this purpose, the emissivity of the samples was measured using the Fourier Transform Infrared spectroscopy (FTIR) using FT/IR-4700 Spectrometer (Jasco). At room temperature, TPU and NBR presented emissivity of 0.89 and 0.85, respectively. Emissivity of the samples was also measured at 125 °C and was noted to remain almost constant. In order to avoid possible errors arising from reflections, all the metallic parts of the test assembly were properly insulated. All the tests were performed at relative humidity levels of 50%.

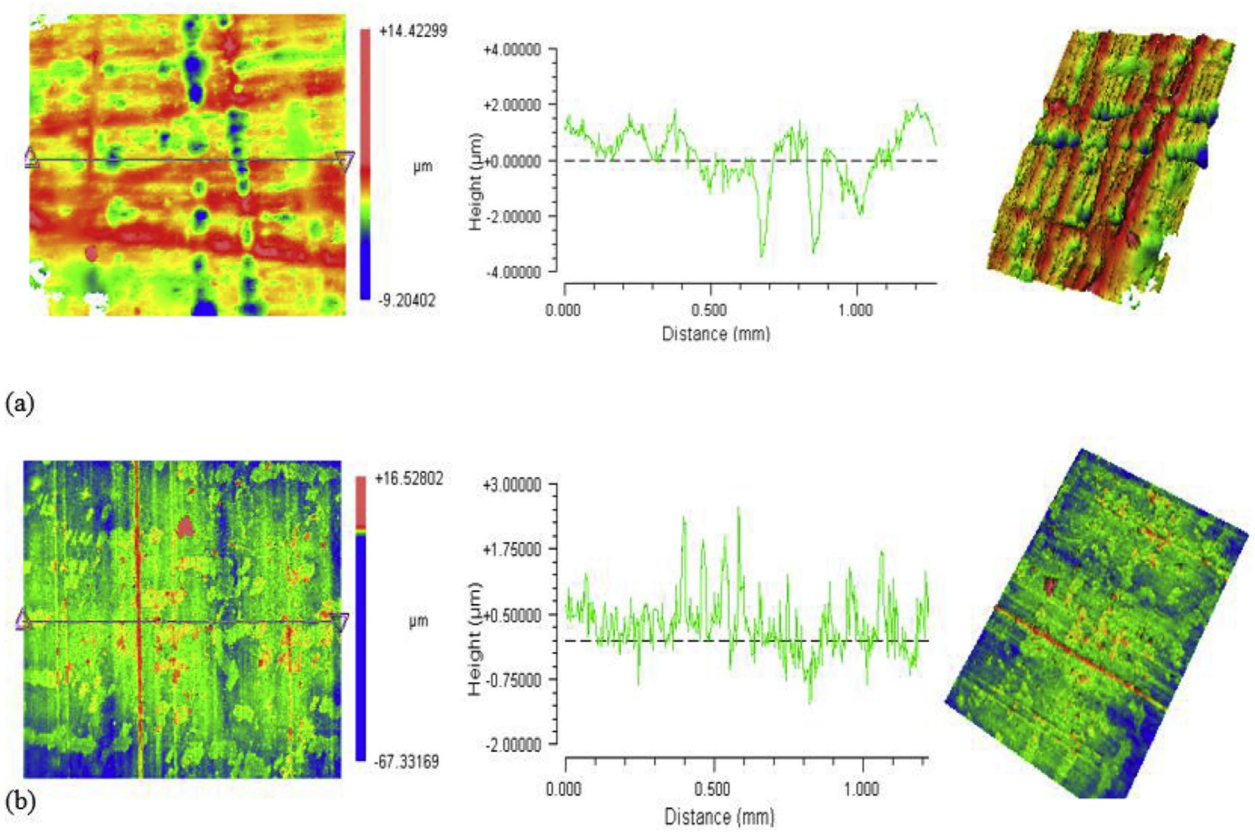

Fig. 3. 3D roughness profile of the reference (a) TPU and (b) NBR samples.

3. Experimental results and discussion

3.1. Friction measurements

The friction coefficient curves obtained from the tribological tests carried out on TPU and NBR samples for different test sliding velocities and cylinder roughness profiles are presented in Fig. 6 and Fig. 7. Regarding the effect of sliding velocity on the friction coefficients recorded, it was found that the friction generated increases with velocity in all the cases. During the running-in period a rapid friction rise occurs due to topographical changes on the surfaces, and this response is faster at high velocities. After this stage a transient zone appears where the friction is maximum, and then friction usually reaches a steady stage. However, results evidence that the behaviour of both elastomers is very different, among others because the tribological response of both samples depend to a great extent on their particular viscoelastic properties (such as hysteresis, stress relaxation and creep, among others). In general, TPU samples led to higher friction coefficients than the NBR samples under the same test conditions. The TPU presented friction coefficient values in the range of 1–1.2 at 0.1 m/s, and approximately

Table 2
Test conditions.

Upper sample	Material	42CrMo4V
	Cylinder length	15 mm
	Cylinder diameter	10 mm
	Cylinder roughness (R_a)	0.1, 0.2 and 0.5 µm
Lower sample	Materials	TPU, NBR
	Polymer sample thickness	5.8 mm
Test conditions	Normal load	15 N
	Stroke length	5 mm
	Oscillation frequency	10 and 25 Hz
	Sliding velocities	0.1 and 0.25 m/s
	Test duration	10 min

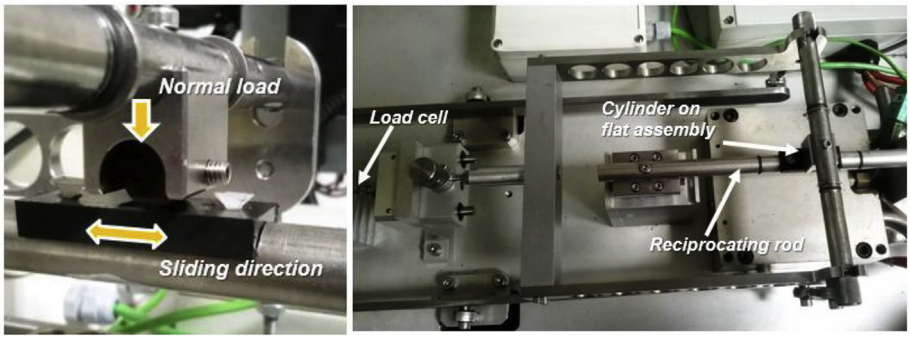

(a) (b)

Fig. 4. (a) Cylinder on flat assembly, (b) test assembly overview.

Fig. 5. TE77 test rig and FLIR SC300 infrared camera assembly.

1.4–1.6 at 0.25 m/s, whereas the NBR presented friction coefficients between 0.8 and 1 at 0.1 m/s, and approximately 1.2 at 0.25 m/s.

Friction coefficient curves of the TPU samples continuously increase with the sliding distance until reaching steady-state values whereas friction curves of the NBR present a peak during the running-in and afterwards decrease until becoming stable. These friction peaks are characteristic of rubber materials and appear during the inception of the relative motion between the mating surfaces [18]. Results also evidenced that the friction curves of the TPU samples are less stable throughout the tests due to stick-slip effects.

Regarding the effect of steel cylinder roughness on friction, in the case of the NBR steel cylinders of 0.1 μm roughness profile are the ones leading to slightly higher friction coefficients under both test velocities. In the case of the TPU samples, however, cylinders with a roughness of 0.5 μm exhibit the highest friction at 0.1 m/s, and those with a Ra of 0.2 μm the highest one during the tests at 0.25 m/s. As sliding velocity increases, the roughness effects become more negligible while the accumulation of thermal effects become more important.

In order to evaluate the effect of the chromium-plating process on friction, Fig. 8 and Fig. 9 present the friction coefficient curves of the elastomeric samples while sliding against both chromed (C) and non-chromed (NC) steel cylinders at different velocities. Results revealed that, in general, chromed cylinders lead to higher friction coefficients than the non-chromed ones during the tests with the TPU samples. This effect, however, is more appreciable within the tests carried out at low velocities and with low roughness cylinder profiles. At 0.1 m/s, and with non-chromed and low roughness (0.1–0.2 μm) cylinders, steady friction coefficients of approximately 1.0 were reached. Under the same conditions but with chromed cylinders, friction coefficients in the range between 1.3 and 1.4 were obtained. It was found that during high velocity tests or/and those tests carried out with cylinders with a R_a roughness of 0.5 μm, test conditions were again so aggressive for the elastomeric samples that the chromium plating process had no significant influence on friction. In the case of the NBR samples (Fig. 9), it was found that the effect of the chromium coating on friction is almost negligible in all the cases.

3.2. Surface temperature measurements

In this section, the surface temperature evolution curves measured on the elastomeric samples are presented together with the calculated friction coefficient curves. Measurements were taken from the interface of the contacting samples in relative motion. A thermal image of the assembly is shown in Fig. 10.

Fig. 11 and Fig. 12 present the variation of friction coefficients and average temperatures at the surface of the TPU and NBR samples during the tests at a velocity of 0.1 m/s. Results showed that the tendencies of the surface temperature curves are similar for both elastomers and under the different test conditions. During the running-in period, the temperatures at the surface of the polymeric samples increase progressively as the friction does, until a near steady state value is reached. Hence, it was found a direct correlation between friction coefficient curves and the measured temperature values. This correlation is in good agreement with the existing analytical models. The temperature curve trends are also in close agreement with those obtained by Tzanakis et al. [12] through in that study tests were performed with PTFE.

Temperature measurements also revealed that the surface temperatures registered at the surface of the TPU samples are higher than

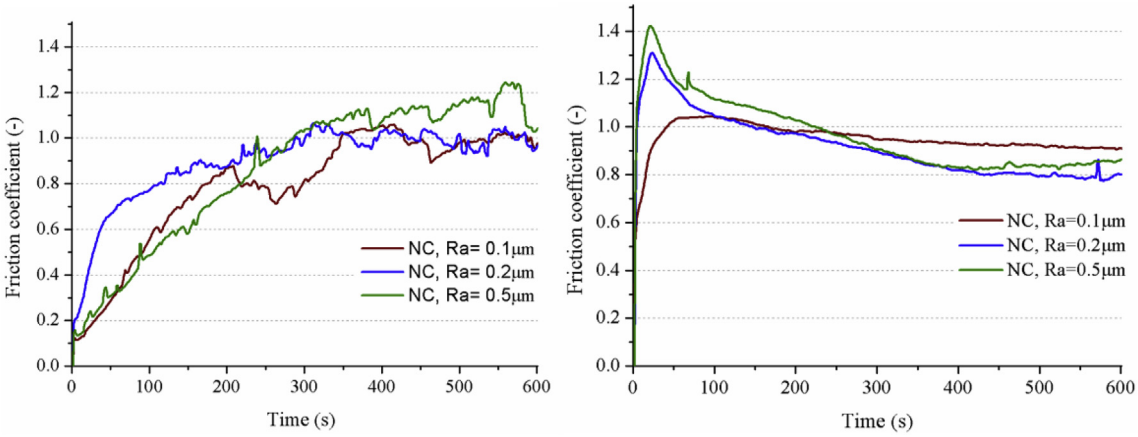

Fig. 6. Friction coefficient curves of Non-Chromed TPU (left) and NBR (right) samples of various roughness at a sliding velocity of 0.1 m/s.

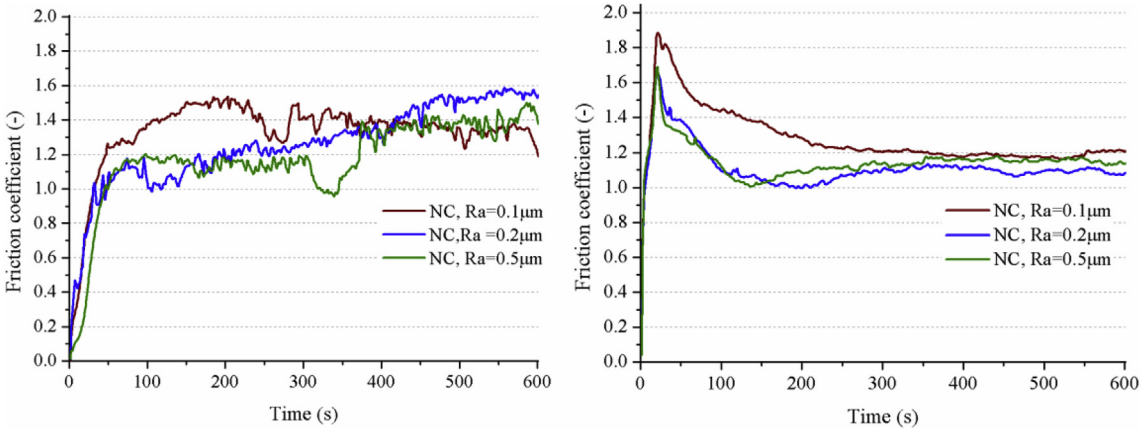

Fig. 7. Friction coefficient curves of Non-Chromed TPU (left) and NBR (right) samples of various roughness at a sliding velocity of 0.25 m/s.

those reached at the surface of the NBR samples under the same conditions. Moreover, large dispersion of the temperature curves with distance in the TPU samples is observed, in the range of 40–60 °C, possibly due to large fluctuations of the friction coefficient. In contrast, in the NBR samples the temperature curves converge to the same temperature range between 40-45 °C having smoother friction coefficient curves.

Results evidenced that the chromium plated (C) surfaces lead to higher temperatures at the surface of the TPU samples than non-chromed (NC) surfaces showing similar tendency to friction. In particular, with chromed cylinders, steady state temperatures between +55 and + 60 °C were registered, whereas with non-chromed cylinders these temperatures were in the range of about +45 °C to +50 °C. Nevertheless, chromium plating does not influence the temperature values measured close to the contact between the steel cylinder and the NBR samples, by contrast. Regarding the effect of roughness on temperature, for both elastomers the highest temperatures were registered for chromed cylinders of 0.1 μm. Nevertheless, it is important to mention that TPU samples are considerably more affected by the roughness of the counterfaces than the NBR ones as also observed for friction.

In general, results do not reveal a clear trend of friction and temperature curves with roughness for this specific case, but they do with the effect of chromium at low test velocities, where it was found that in general it increases both the friction and temperature on both NBR and TPU.

In Fig. 13 and Fig. 14 friction coefficient and average surface temperature curves are presented as a function of the sliding distance for a velocity of 0.25 m/s. A good agreement between friction and thermal results was also found in this case. Results showed that at this velocity more time is required to reach a steady-state temperature regime than at lower velocities, mainly due to the instabilities presented by the friction curves. The TPU presented stable temperatures in the range of +66 °C and +77 °C in all the cases, and it was found that the effect of surface conditions of the steel parts on the temperatures reached on the TPU samples is almost negligible. In the case of the NBR, under steady-state conditions, all the tribo-pairs showed similar temperature values in the range of +55 and + 60 °C. In general, at this velocity it is difficult to establish any relation between the surface conditions of the steel cylinders, the friction and temperature. As Blau et al. reported in Ref. [21], in some cases wear quickly alters the contact surfaces so that any attempt to correlate the frictional performance with the initial surface conditions may be inappropriate.

Regarding the effect of velocity on temperature, the TPU samples presented, surface temperatures between +40 °C and +60 °C at 0.1 m/s, and temperatures between +60 °C and +77 °C to 0.25 m/s. In the case of the NBR samples, they presented surface temperatures between +40 °C and +45 °C at 0.1 m/s, and between +56 °C and +62 °C at 0.25 m/s. Here, the experimental study on the frictional heating within elastomers is influenced more by velocity than by the steel counterface characteristics. Furthermore, it can be also observed that the NBR samples presented lower friction and surface temperature values than the TPU samples under the different test conditions. The friction curves of the rubber samples were more stable in all the cases than the curves obtained with the polyurethane materials. It is thought that the main reason for those instabilities in the friction curves of the TPU samples may be the high hardness of the material (93 Shore A).

In general, the frictional heat generated during sliding results in two antagonistic effects on the friction coefficient. On the one hand the shear strength of the elastomers decreases and so does the friction coefficient. On the other hand, the elastic modulus of the composite decreases, assisting the formation of multiple adhesion joints by the asperities impaction which resulted in more contact spots due to the larger contact area and then the associated friction coefficient increase. Therefore the resultant friction coefficients are determined by these two competitive aspects [20].

Another important factor for the frictional heating investigation is the temperature reached in the bulk of the tested samples. Fig. 15 presents the evolution of the temperature in the bulk of the elastomers during the tests. These temperatures were measured at the centre of the contact of the elastomeric samples at a distance of 4 mm from the surface. Measurements demonstrate that the bulk of the tested elastomers is also affected by the frictional heating, not only the surface. As can be seen, bulk temperatures increase gradually during motion until reaching steady temperature conditions. These results are in good agreement with Tian and Kennedy [7,8], who found that in the case of bodies with a finite thickness subjected to heat sources moving over the same path continuously, there is a temperature rise known as nominal temperature rise that affects the entire contact area. Moreover, results revealed that the temperatures reached in the bulk of the NBR samples are higher than those measured in the TPU samples while the surface temperatures were higher on the latter. The main reason is that the thermal diffusivity of the NBR is higher so that the heat moves more rapidly (see Fig. 2). Additionally, the temperature inside the samples stabilises faster during the tests carried out at low velocity (0.1 m/s) rather than at those performed at higher velocities (0.25 m/s), where temperatures did not reach a steady value even if friction and contact temperature did as shown in Fig. 15.

3.3. Wear and surface observations

In order to evaluate the wear mechanisms of the elastomers, SEM micrographs were taken and analyzed. Fig. 16 presents the surface profiles of the elastomeric samples, before and after the tests. As can be

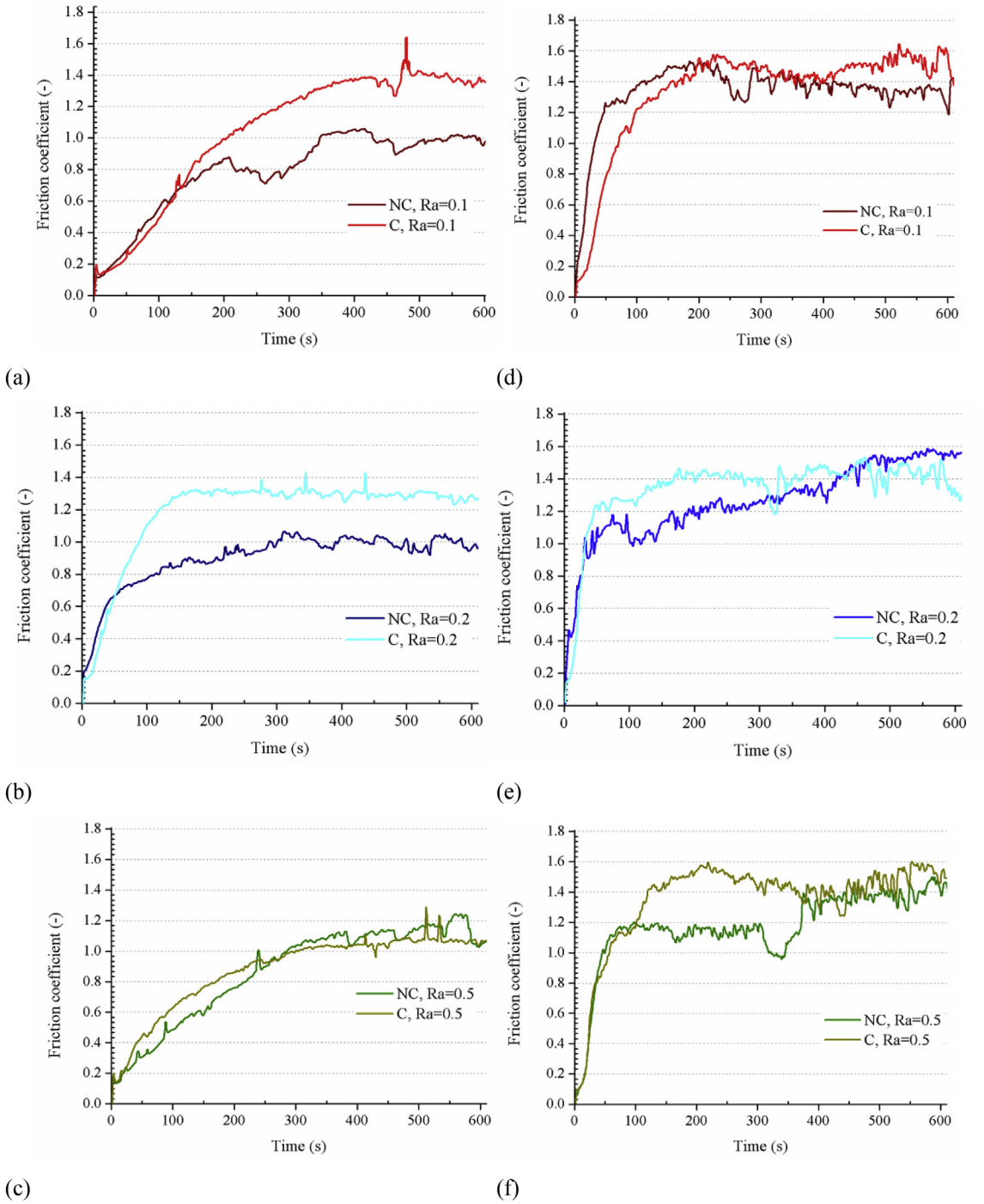

Fig. 8. Effect of the chromium-plating process on the friction of the TPU samples at 0.1 m/s (a, b, c) and at 0.25 m/s (d,e,f).

seen, Schallamach waves are present within all the wear scars. These waves are characteristic of rubber-like materials and its stick-slip motion, and they are oriented perpendicularly to the sliding direction since they are the result of periodic fluctuations between compression and tension along the contact surface. In other words, Schallamach waves are the result of consecutive contact adhesions occurring at the surface during sliding due to the visco-elasticity of elastomers and their ability to extend giving local recoverable strains [16].

In order to evaluate the wear of the samples, their mass was measured before and after each test. Confocal microscopy was used for mass loss visualization and profile measurements of the wear scars (Fig. 17). Results evidence that the applied load is distributed in a different way in both elastomers, thus, their wear scar profile is also different. As can be observed, the depths of the wear scars of the NBR samples are considerably bigger than those of the TPU samples (more than 3 times). Furthermore, TPU samples tend to wear more at the extremes of the wear scar rather than at the centre.

In order to compare the samples from a tribological point of view, both friction coefficients and wear rates need to be considered because samples exhibiting the same friction may present very different wear rates depending on how the energy is partitioned within and between the rubbing material surfaces. Thus, Fig. 18 presents the frictional energy of the samples under different test conditions compared with the mass loss. In particular, three values have been plotted per test condition, one for each cylinder roughness. The specific wear energy can be calculated as the ratio of the friction work to the mass loss due to wear

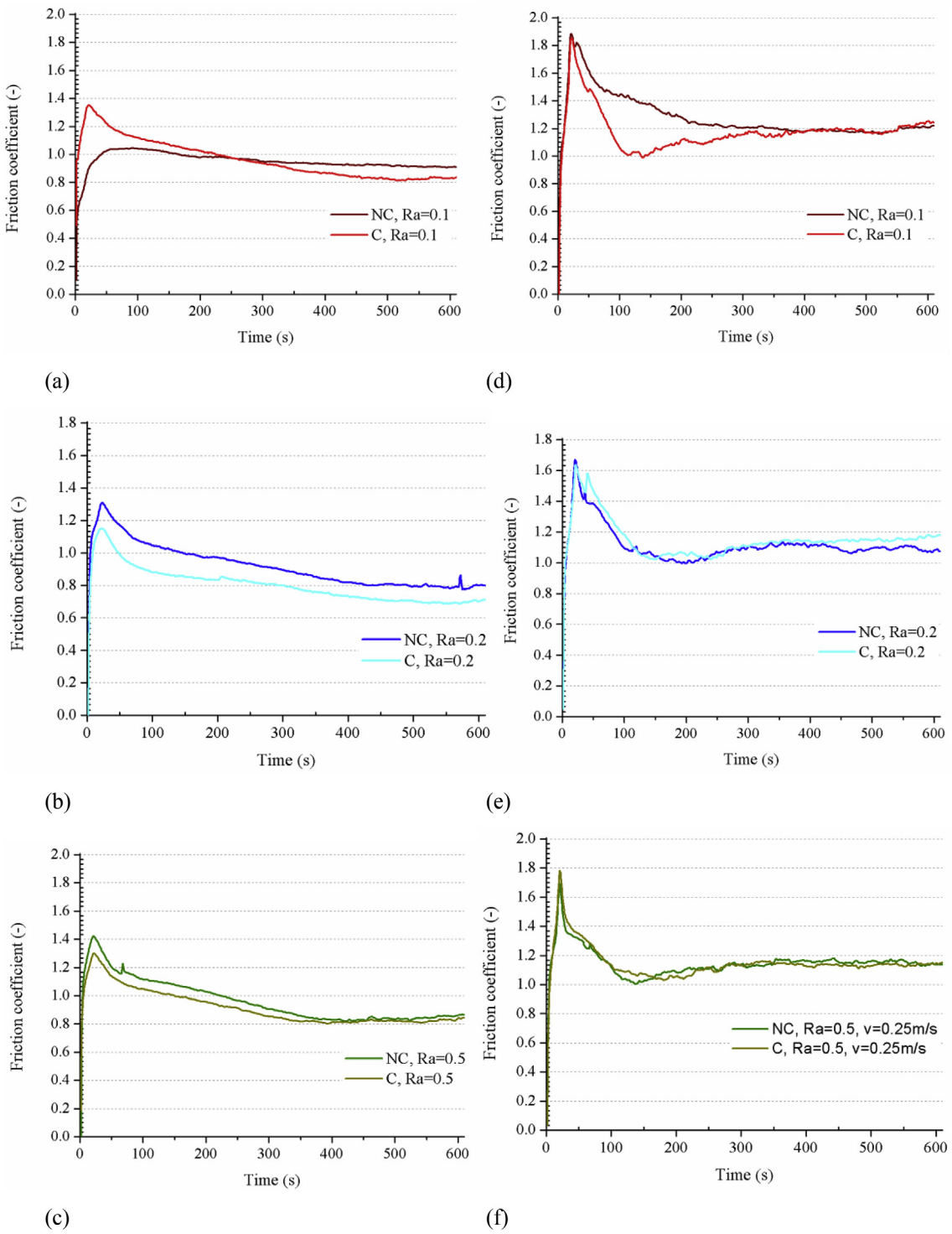

Fig. 9. Effect of the chromium-plating process on the friction of the NBR samples at 0.1 m/s (a, b, c) and at 0.25 m/s (d, e, f).

(Eq. (2)):

$$E_w = \frac{E}{\Delta m} = \frac{v\,N\int_{ti}^{tf}\mu(t)dt}{\Delta m} \quad (2)$$

where E_w is the specific wear energy, E is the energy dissipated by friction, v is the mean relative sliding velocity, N is the normal load, μ is the coefficient of friction, ti the initial time, tf is the time at the end of the test, and Δm is the total mass loss. As can be seen, both materials present similar frictional energy at every velocity, however, the specific wear energy of the TPU is considerably higher i.e. the abrasive resistance of the TPU is considerably higher under the selected test conditions since it requires more energy to be worn out than the NBR.

4. Analytical flash temperature calculations

In this section different temperature analytical models were applied to investigate the capability of these models to predict the temperatures reached at the contact of the tested elastomers, and for the considered test conditions. Contact temperatures were theoretically calculated and compared with the experimental values measured using the thermo-

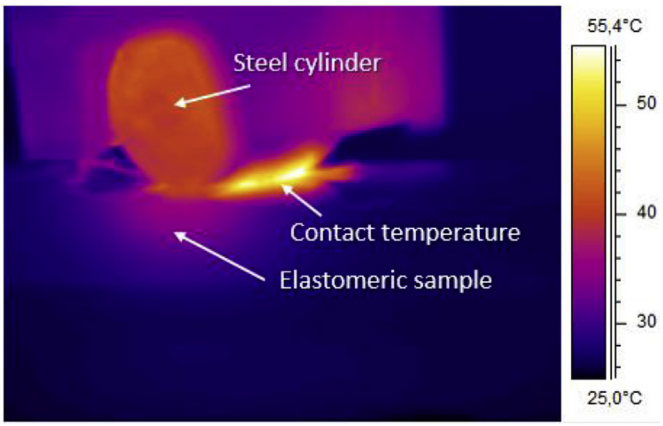

Fig. 10. Thermal image example from the tribo-system.

camera. The temperature at the contact (Eq. (3)) is expressed as the sum of two components [19]:

$$T_{cmax} = T_b + T_{fmax} \tag{3}$$

where T_{cmax} is the maximum contact temperature [°C], T_b is the bulk temperature of the mating bodies before entering the contact [°C] and T_{fmax} is the temperature rise that takes place at the contact spots [°C] which is a local temperature rise that occurs between asperities. However, Equation (2) is only applicable to a body with a semi-infinite size, and when the heat source does not repeat the same path over the surface so that there is no heat storage within the body. Tian, Kennedy et al. [7,8], found that under certain circumstances an additional temperature rise over the localized flash surface temperature rise at the contacting asperities must be considered. This temperature rise will affect the entire contact area and it is known as "nominal contact temperature". Some examples in which this nominal temperature rise should be considered include cases such as: when the heat source moves continuously over the same path of a finite body, when there is insufficient convective cooling, or/and under dry sliding conditions. Thus, the local surface temperature rise is only affected by a small area while the nominal temperature rise affects the entire finite body. Taking into account these aspects, the temperature at the contact may be expressed theoretically as (Eq. (4))

$$T_c = T_b + \Delta T_{nom} + \Delta T_f \tag{4}$$

where ΔT_{nom} as the average temperature of all the points at the contact, ΔT_f as the flash temperature rise that takes place at the contact asperities and T_b as the environment temperature. The existing theoretical models are based on different assumptions, they all assume steady and quasi-steady conditions since they consider that the maximum flash temperatures are reached in a very short time after sliding initiates.

The heat rate "q" originated during sliding can be estimated as follows:

$$q = Q/A \tag{5}$$

where Q is the heat generated and A is the contact area.

Considering that the origin of this heat flux is the relative motion between the bodies A and B, the frictional heat generated may be expressed as:

$$Q = \mu F_N |v_A - v_B| \tag{6}$$

where μ is the friction coefficient between surfaces, F_N is the normal load, and v_A and v_B are the sliding velocities of the bodies A and B, respectively.

It is already known that temperature rise calculations depend up to a great extent on the considered real contact area, friction coefficients and thermal properties [9]. Even if a broadly accepted criteria set considers the calculation of the real contact area by dividing the load by the hardness of the softer material, in this case this criterion is not applicable since the hardness of elastomers must be measured by means of Shore A and Shore D durometers. Hence, even if in Ref. [12] some authors used the Bowden and Tabor model for theoretical calculations of the contact temperature on PTFE (polyfluorethylene), this could not be applied in this study as it involves introducing the hardness of the softer material which is not applicable for elastomers. Hence, in this investigation, two of the most popular analytical models have been applied for flash temperature calculations: Jaeger model [5] and Tian & Kennedy model [8]. The equations of these models are shown in Table 3. It is important to highlight that the Jaeger equations estimate the average flash temperature along the contact area whereas Tian & Kennedy's equations predict the maximum one. Both models were applied in order to find out which model performs better for these particular test conditions and materials. Most of the analytical models use different formulations depending on the velocity regime. For determination of the velocity regime [19], the dimensionless "*Peclet number, Pe*" is used which is an indicator of the heat penetration into the bulk of the solid and could be expressed as $Pe = {}^{vb}/_{2\chi}$.

Here the contact width $2b$ was measured at the end of each test and those values were considered for calculations (Table 4). The theoretical models assumed that the real contact area is similar to the apparent contact area. This assumption is justified since the materials under study are elastomers. For calculations, the friction coefficient evolution measured during the tests was used and the thermal properties from Fig. 2 were considered. In Ref. [14] it was demonstrated the importance of taking into account the variation of material thermal properties with temperature, however, in this case some calculations were performed

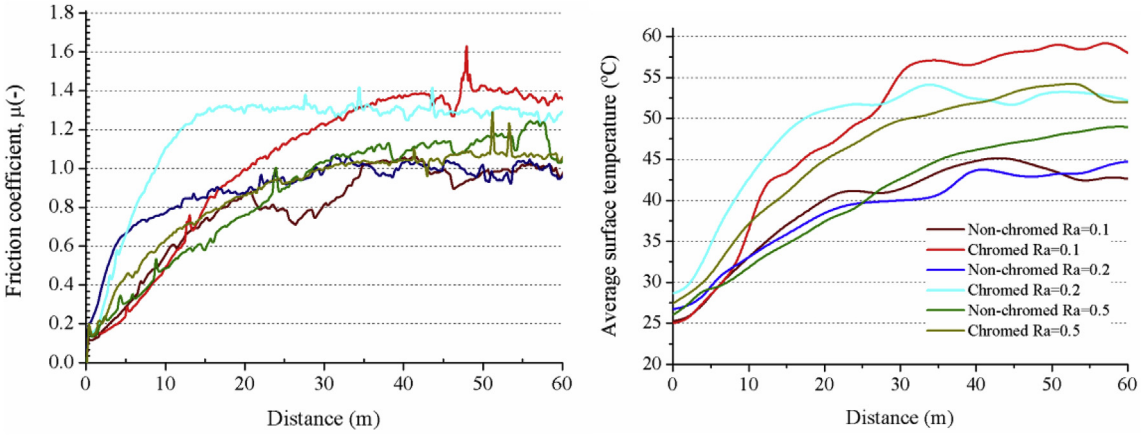

Fig. 11. Friction and temperature curves of the TPU samples sliding against steel mating surfaces with different roughness and surface conditions at 0.1 m/s.

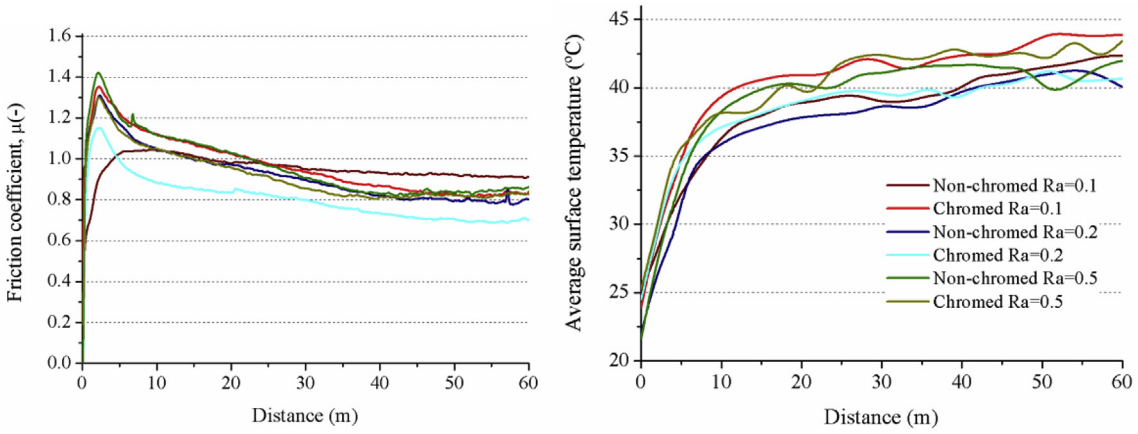

Fig. 12. Friction and temperature curves of NBR samples sliding against steel mating surfaces with different roughness and surface conditions at 0.1 m/s.

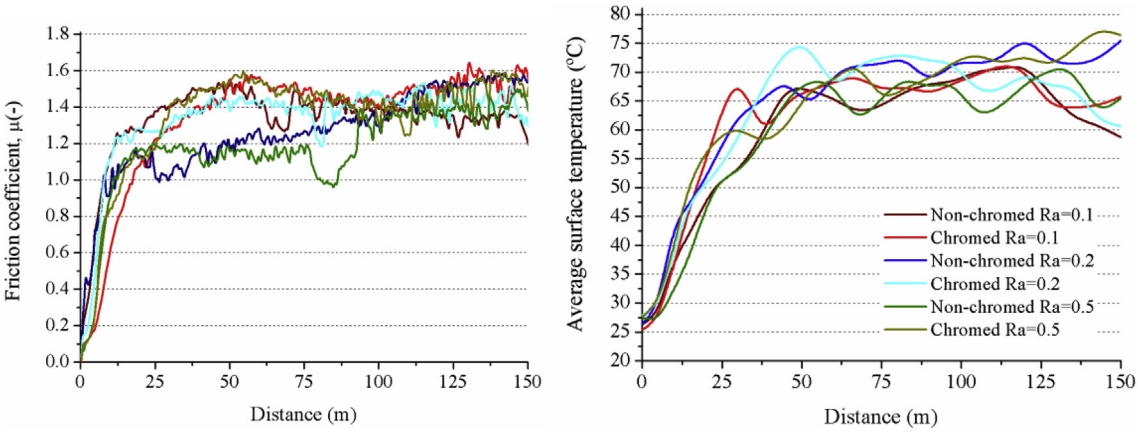

Fig. 13. Friction and temperature curves of the TPU samples sliding against steel mating surfaces with different roughness and surface conditions at 0.25 m/s.

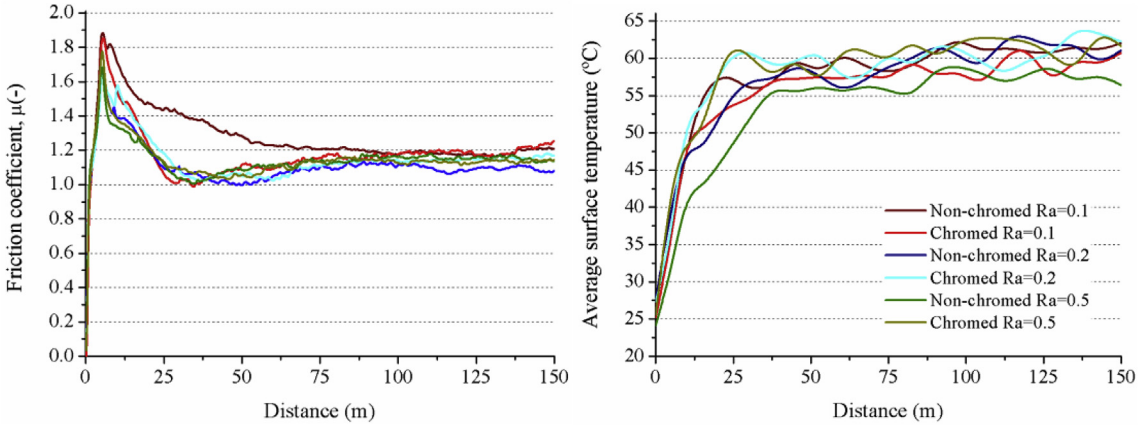

Fig. 14. Friction and temperature curves of the NBR samples sliding against steel mating surfaces with different roughness and surface conditions at 0.25 m/s.

and it was found that thermal properties variation is so small within the operating temperature range that it does not significantly influence the results.

Fig. 19 presents a comparison between the flash temperatures calculated analytically applying the equations in Table 3 and those values calculated from the experimental data. The experimental flash temperature curves have been calculated indirectly as the difference between the surface temperatures and those temperatures measured in the bulk (Eq. (7)):

$$T_{f.exp} = T_{surf} - T_{bulk.exp} \quad (7)$$

where T_{surf} is the temperature measured at the surface of the elastomers through the infrared camera, $T_{bulk.exp}$ is the bulk temperature of the elastomer experimentally measured and $T_{f.exp}$ is the experimental flash temperature.

In general, a good agreement was found between the experimental flash temperature curves and the analytical curves calculated using the model of Tian & Kennedy for maximum flash temperature calculations [8]. Hence, it was found that Tian & Kennedy's model shows a better fit in comparison with Jaeger which approximates the flash temperatures reached at the surface of the TPU and NBR elastomers under the studied operating conditions. Furthermore, results revealed that a better

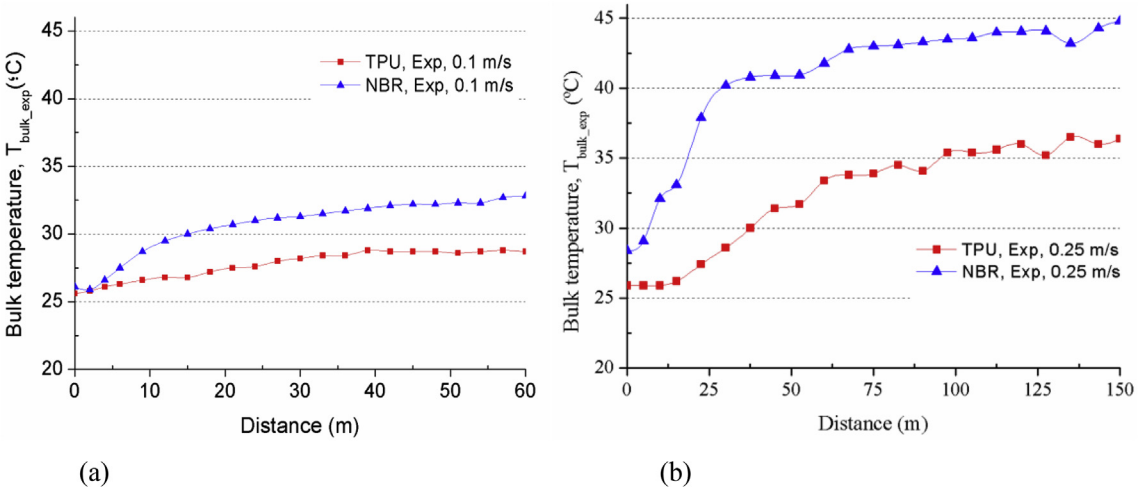

Fig. 15. Temperature measurement in the bulk of the elastomeric samples throughout the tests: (a) at 0.1 m/s and (b) at 0.25 m/s.

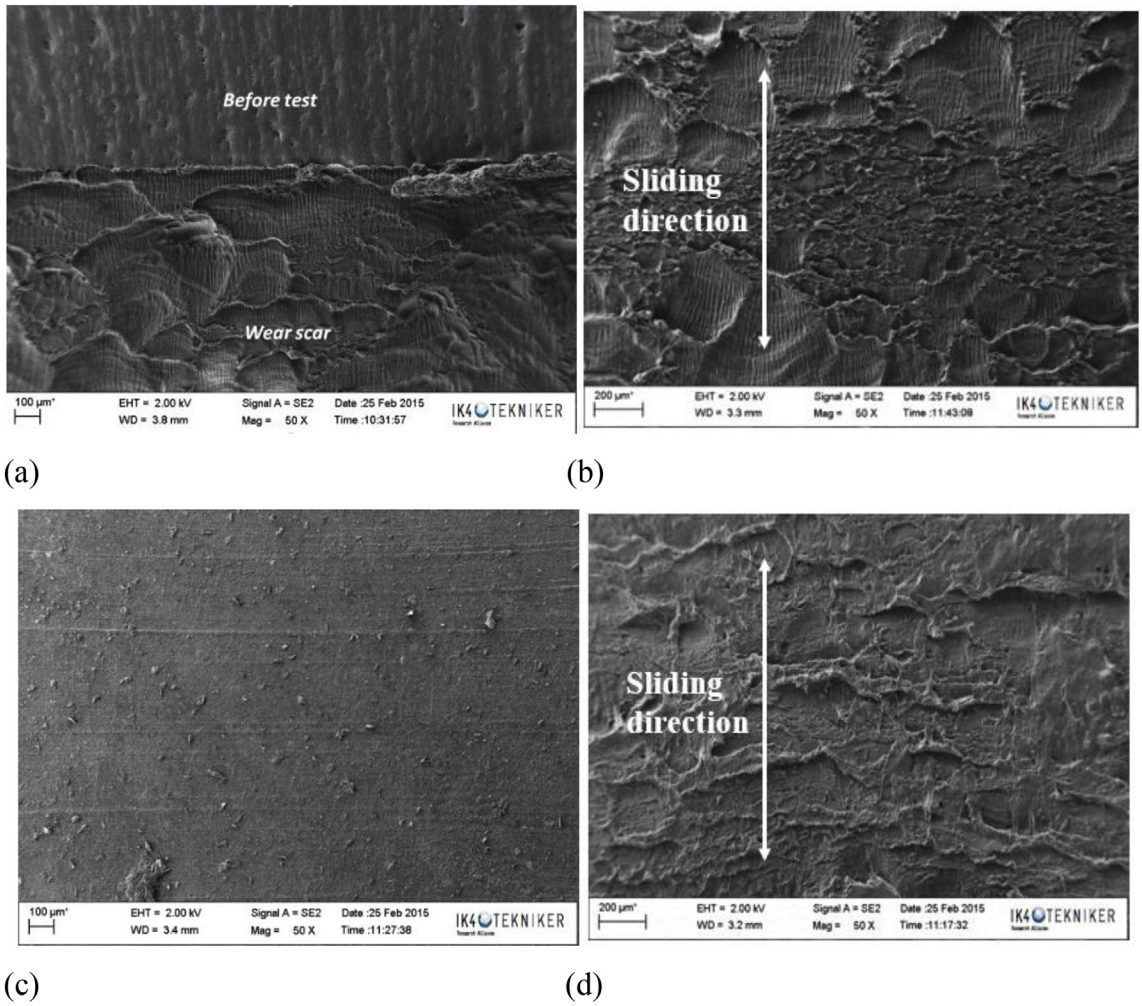

Fig. 16. TPU surface (a) before and (b) after the tests, and NBR surface (c) before and (d) after the tests.

matching was achieved at low velocity conditions.

5. Conclusions

Temperature rise during operation is especially important in applications dealing with elastomers due to their limited thermal resistance. The aim of this research was to carry out an experimental investigation on the influence of frictional heating on the temperature rise and tribological behaviour of TPU and NBR elastomers. The main conclusions of the investigation can be summarized as follow:

- The frictional behaviour of both elastomers is completely different. In general, TPU presents higher friction coefficients under the same conditions and less stable friction curves due to stick-slip effects.

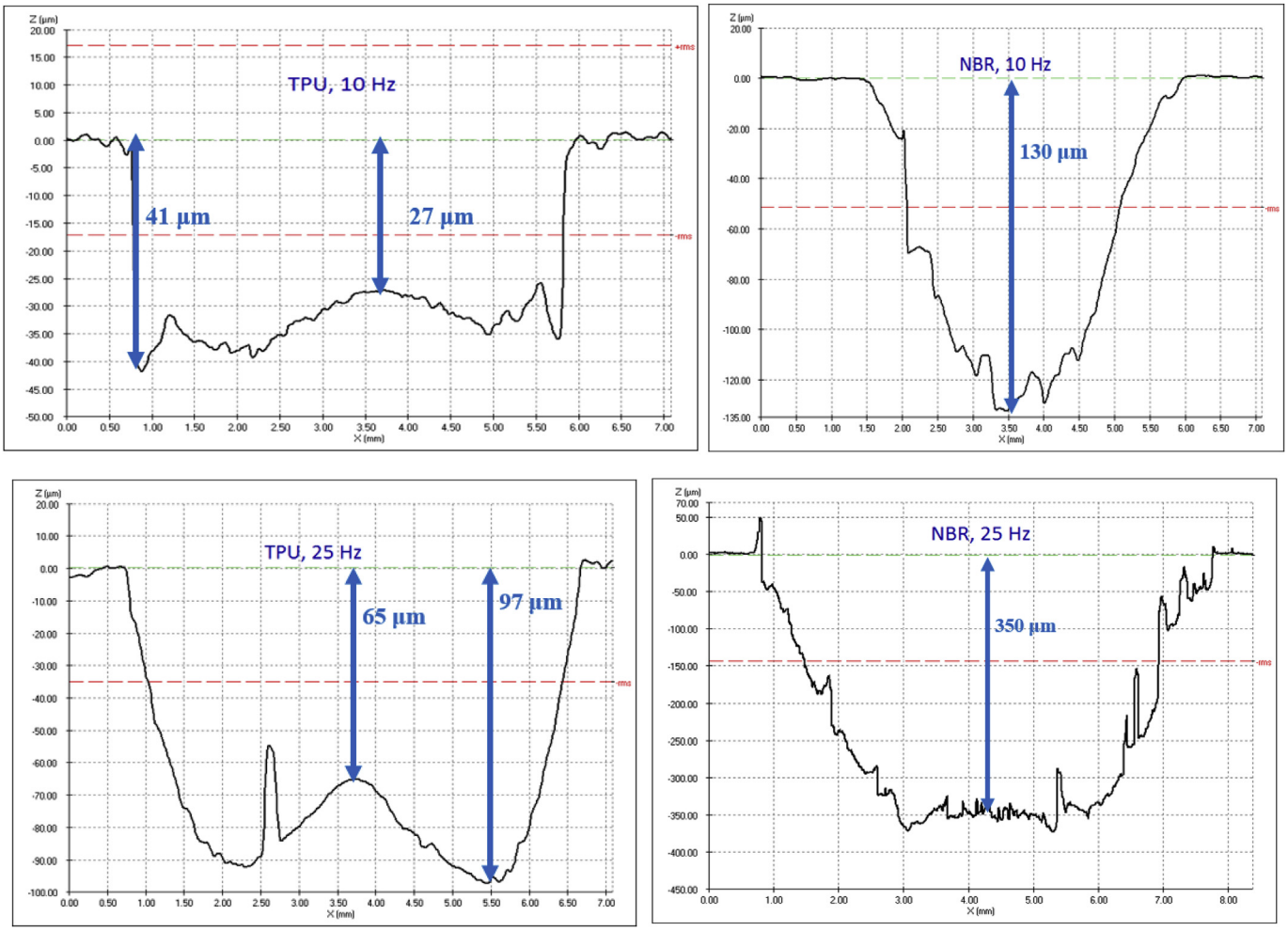

Fig. 17. Micrographs of the wear scars under different conditions.

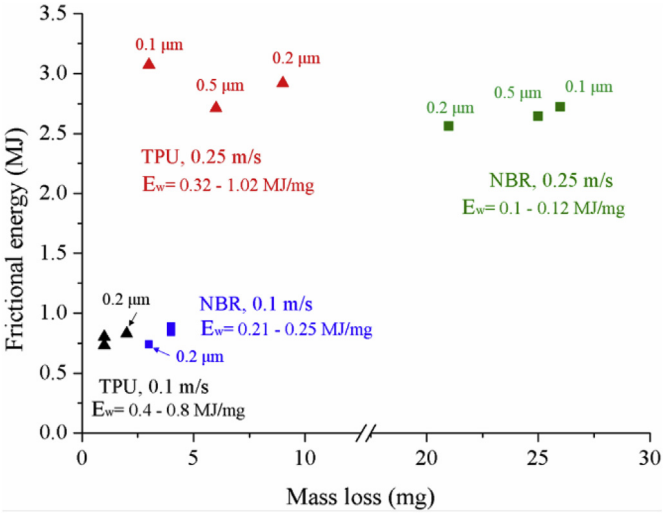

Fig. 18. Frictional energy vs mass loss.

Table 3
Analytical models for flash temperature calculations.

Model	Equation	
Jaeger (1942)	Stationary or low speed Pe < 0.1	$T_{fave} = 0.946 \frac{q\,b}{k}$
	Moving Pe > 10	$T_{fave} = \frac{1.064\,q}{k}\left(\frac{X\,b}{v}\right)^{1/2}$
Tian & Kennedy (1994)	Stationary or low speed Pe < 0.1	$T_{fmax} = \frac{2\,q\,b}{k\sqrt{\pi}}$
	Moving Pe > 10	$T_{fmax} = \frac{2\,q\,b}{k\sqrt{\pi\,Pe}}$

Table 4
Contact widths of the wear scars.

	Contact width, 2b (mm)	
	0.1 m/s	0.25 m/s
TPU	4.1	6.3
NBR	4.5	7.2

- Friction coefficient and temperature curves tend to stabilize almost simultaneously, showing the surface temperature association with the generated frictional energy.
- Even if the frictional energy generated on both elastomers is similar, the way of dissipating this energy differs. In general, the temperatures reached at the surface of the TPU are higher whereas the heat accumulation in its bulk is lower than in the case of the NBR. Wear energy of the TPU is about four times that of the NBR i.e. the abrasive resistance of the TPU is higher under the selected test conditions.
- Sliding velocity is the most influential parameter affecting the temperature rise on elastomers. The effect of surface conditions

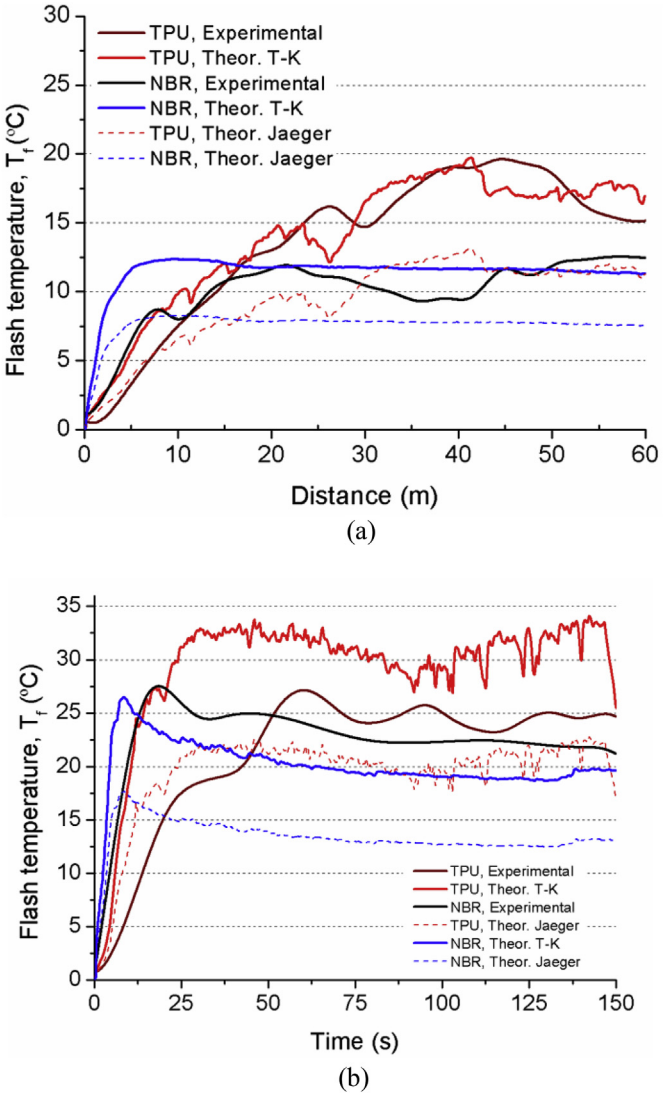

Fig. 19. Comparison between experimental and analytical flash temperature curves obtained with chromed cylinders with R_a = 0.1 μm at (a) 0.1 m/s and (b) 0.25 m/s.

becomes negligible as the test velocity rises.

- Good correlation was found between experimental temperature measurements and the values calculated theoretically using the equations suggested by Tian&Kennedy. The theoretical predictions, however, become less accurate as the sliding velocity decreases.
- Jaeger flash temperature model underestimates the temperatures reached at the interface between sliding bodies for the elastomers under study and the selected test conditions.

Viscoelasticity of the materials under test and its dependence on temperature is still a topic under study as well as its influence on tribological characteristics. Future developments may address the research on the effect of viscoelastic properties on the frictional heating.

Acknowledgements

The authors would like to thank the EPSRC Engineering Instrument Pool in the UK for the loan of the infrared camera used for temperature measurements.

References

[1] Pinedo B, Conte M, Aguirrebeitia J, Igartua A. Effect of misalignments on the tribological performance of elastomeric rod lip seals: study methodology and case study. Tribol Int 2017;116:9–18.
[2] Kalin M. Influence of flash temperatures on the tribological behaviour in low-speed sliding: a review. Mater Sci Eng, A 2004;374:390–7.
[3] Kennedy FE, Frusescu D, Li J. Thin film thermocouple arrays for sliding surface temperature measurement. Wear 1997;207(1–2):46–54.
[4] Kennedy FE, Tian X. The effect of interfacial temperature on friction and wear of thermoplastics in the thermal control regime. Dissipative processes in Tribology. Elsevier Science; 1994.
[5] Jaeger JC. Moving sources of heat and the temperatures at sliding contacts. J Proc Soc N.S.W 1942;76:205–24.
[6] Blok H. The dissipation of frictional heat. Appl Sci Res A 1955;5(2):151–81.
[7] Tian X, Kennedy FE. Contact surface temperature models for finite bodies in dry and boundary lubricated sliding. J Tribol 1993;115.
[8] Tian X, Kennedy FE. Maximum and average flash temperatures in sliding contacts. J Tribol 1993;116.
[9] Kalin M, Vizintin J. Comparison of different theoretical models for flash temperature calculation under fretting conditions. Tribol Int 2001;34:831–9.
[10] Wieleba W. The role of internal friction in the process of energy dissipation during PTFE composite sliding against steel. Wear 2005;258:870–87.
[11] Rowe K, Bennett A, Krick B, Gregory Sawyer W. In situ thermal measurements of sliding contacts. Tribol Int 2013;62:208–14.
[12] Tzanakis I, Conte M, Hadfield M, Stolarski TA. Experimental and analytical thermal study of PTFE composite sliding against high carbon steel as a function of the surface roughness, sliding velocity and applied load. Wear 2013;303:154–68.
[13] Conte M, Pinedo B, Igartua A. Role of crystallinity on wear behaviour of PTFE composites. Wear 2013;307:81–6.
[14] Conte M, Pinedo B, Igartua A. Frictional heating calculation based on tailored experimental measurements. Tribol Int 2014;74:1–6.
[15] Conte M, Pinedo B, Igartua A. Frictional heating calculations for polymers. Proceedings of the surface effects and contact mechanics XI Congress – Siena, Italy. 2013.
[16] Stachowiak GW. Wear: materials, mechanisms and practice. Wiley; 2005.
[17] Kim H, Kim R-U, Chung K-H, et al. Effect of test parameters on degradation of polyurethane elastomer for accelerated life testing. Polym Test 2014;40:13–23.
[18] Bhushan B. Adhesion and stiction: mechanisms, measurement techniques and methods for reduction. J Vac Sci Technol B 2003;21(6).
[19] Stachowiak GW, Batchelor AW. Engineering Tribology. Butterworth-Heinemann; 2005.
[20] Abdelbary A. Wear of polymers and composites. Woodhead Publishing, Elsevier; 2014.
[21] Blau Peter J. Friction Science and technology: from concepts to applications. second ed. STLE. CRC Press Taylor & Francis Group; 2009.